Postprint of: Pancielejko A., Mazierski P., Lisowski W., Zaleska-Medynska A., Kosek K., Łuczak J., Facile formation of self-organized TiO2 nanotubes in electrolyte containing ionic liquid - ethylammonium nitrate and their remarkable photocatalytic properties, ACS Sustainable Chemistry & Engineering, Vol. 6, iss. 11 (2018), pp. 14510-14522,
DOI: 10.1021/acssuschemeng.8b03154

This document is the Accepted Manuscript version of a Published Work that appeared in final form in **ACS Sustainable Chemistry & Engineering**, copyright © American Chemical Society after peer review and technical editing by the publisher. To access the final edited and published work see https://pubs.acs.org/doi/10.1021/acssuschemeng.8b03154

Facile formation of self-organized TiO_2 nanotubes in electrolyte containing ionic liquid - ethylammonium nitrate and their remarkable photocatalytic properties

Anna Prochownik[a], *Paweł Mazierski*[b*], *Wojciech Lisowski*[c], *Adriana Zaleska-Medynska*[b], *Klaudia Kosek*[d], *Justyna Łuczak*[a*]

[a]Department of Chemical Technology, Faculty of Chemistry, Gdansk University of Technology, G. Narutowicza 11/12, 80-233 Gdansk, Poland

[b]Department of Environmental Technology, Faculty of Chemistry, University of Gdansk, Wita Stwosza 63, 80-308 Gdansk, Poland

[c]Institute of Physical Chemistry, Polish Academy of Science. Kasprzaka 44/52, 01-244 Warsaw, Poland

[d]Department of Analytical Chemistry, Faculty of Chemistry, Gdansk University of Technology, G. Narutowicza 11/12, 80-233 Gdansk, Poland

Corresponding Authors

J. Łuczak: E-mail: justyna.luczak@pg.gda.pl

P. Mazierski: E-mail: pawel.mazierski@phdstud.ug.edu.pl

ABSTRACT

The oriented TiO_2 nanotube arrays (NTs) are identified as a stable, active and recyclable photocatalytic surface. However, their photoactivity is strictly depended on morphology (especially length), which could be controlled by anodic oxidation parameters, including electrolyte properties. To control the morphology, were successfully synthesized a series of NTs by a novel approach where ionic liquid (IL), ethylammonium nitrate [EAN][NO_3], was used as an addition to an organic electrolyte. Using scanning electron microscopy, X-ray diffraction, X-ray photoelectron spectroscopy, diffuse reflectance UV-Vis spectroscopy and photoluminescence spectroscopy we are able to show how electrolyte composition influence nanotubes surface properties and photocatalytic activity. It was found that the change in the amount of [EAN][NO_3] in electrolyte used for anodization in the range from 0.05 to 1.0 wt.% affected dynamic viscosity, conductivity and surface tension of electrolyte and finally alter morphology of formed nanotubes resulting in a proportional increase of the outer diameter and tube length from 105 to 140 nm and from 6.0 to 8.1 μm, respectively. The highest photoactivity (achieving high reaction rate constant, equal to $k = 0.0941\ min^{-1}$) and wettability was found for the sample prepared in the electrolyte containing 0.05 wt.% of [EAN][NO_3] revealing the improved ability to light photoabsorption and suppression of recombination rate. It turned out that IL_NTs surface became more hydrophobic when stored in air ambience over 7 weeks after fabrication with approximately 20 – 52°. The increase of the contact angle from 9.3 to 13.1° with elongation of the tube diameter from 107 to 140 nm was also noted.

KEYWORDS: TiO_2 nanotubes; ionic liquid; electrochemical method; anodization, phenol degradation; photoactivity; photocatalysis.

INTRODUCTION

Titanium dioxide (TiO_2) thin films in a form of nanotubes (NTs) have gained considerable

MOST WIEDZY Downloaded from mostwiedzy.pl

attention due to their properties meeting requirements stated materials that are used for air and water streams purification and disinfection[1], water splitting[2], exhaust gases monitoring[3], dye-sensitization[4], controlling the surface wettability[5] or drug delivery[6–8]. The main predominance of these structures over the nano- and microsized powders is formation of oxides layers deposited onto the solid substrate that are easy to handle[9]. In this regard, thin films do not require separation from the reaction environment, minimizing the operational costs.

One-dimensional (1D) TiO_2 nanotube layers on a Ti surface can be formed by various methods among which sol-gel techniques[10], hydro/solvothermal[11], atomic layer deposition into the template[12], and electrochemical methods[13] are the most popular. Anodic oxidation of metallic titanium substrate in an electrolyte with proper composition and under specific electrochemical conditions provided well-ordered, dense, aligned array of TiO_2 NTs with high surface area to volume ratios, desirable electronic properties and even high mechanical strength[9]. Moreover, the advantages of the electrochemical method are also related with (i) low processing temperature, (ii) relatively low investment and operational costs, (iii) simple performance, (iv) ability to control preparation rate, thus pore size, length, and wall thickness, and (v) possibility to apply thin film to a surface with virtually any complicated shape and structure (thus easy to scale up)[9,14].

Dimensionality of NTs was found to be a crucial factor determining the electronic properties (electron mobility, quantum size effects) of the tubular material. Therefore, the control of size and shape of NTs is of great interest and may improve interaction between a device and the surrounding media. Consequently, such systems may work more effectively or allow for novel reaction pathways. In this regard, the length of the TiO_2 self-organized layers is usually adjusted mainly by applied voltage and also by selection of the anodization time and etching rate[15,16]. Geometry of the NTs can be also improved by modification of the electrolyte composition. Almost ideal hexagonally ordered arrays can be obtained in electrolyte composed of ethylene

MOST WIEDZY Downloaded from mostwiedzy.pl

glycol (EG) containing fluoride species (HF[17], NH_4F, NaF[18]), however other solvents, such as ionic liquids[13] (ILs) and acetic acid[19], were also proposed. Interesting and giving a new possibilities could be use of IL as an electrolytes[13,20] and additives to traditional electrolytes[21]. Ionic liquids, being a group of salts composed of ions with melting point below 100°C, have gain particular attention in the area of various nanomaterials synthesis[22,23]. In view of their unique properties such as low vapour pressure, chemical and thermal stability, high conductivity, polarity, non-flammability and good dissolving properties, ILs were found to be attractive media used as solvents, structuring agents or temples for nanostructures[22]. Up to date, in synthesis of NTs, ILs were successfully used as electrolyte[13] or component of the electrolyte[24]. The first study on the anodization of Ti, performed in 1-butyl-3-methylimidazolium tetrafluoroborate [BMIM][BF_4] ionic liquid, was published by Paramasivam *et al.*[13]. It was shown that anodization in the range of 5 - 10 V in time 1, 5 and 10 h provided well-defined layers of NTs with the length being in the range of 340 - 650 nm and diameter between 27 and 43 nm[13]. Surprisingly, during synthesis in the other easily hydrolysable IL, 1-butyl-3-methyl-imidazolium hexafluorophosphate [BMIM][PF_6], NTs were not formed[13]. The improvement of the titanium foil anodization process in the [BMIM][BF_4]-based electrolytes was performed by Li *et al.*[25]. With increasing the anodization potential the dimensional parameters of NTs, length and diameter, grown from 0.9 μm and 70 nm (at 10 V) up to 4.5 μm and 400 nm (at 50 V), respectively. The same ionic liquid was also used as an additive to an electrolyte composed of ethylene glycol and water by Wender *et al.*[26]. The length and diameter of NTs layers grown up to 6.3 μm and 400 nm, respectively, during anodization in the range of 20 – 100 V with addition of water (0 – 30 vol.%). Water content was defined as a meaningful parameter in formation of NTs, up to 10%[26], providing longer and wider nanostructures. The effect of the IL's cation structure (used as a component of the glycol-based electrolyte) and its content on the geometry of NTs was for the first time reported by our

MOST WIEDZY Downloaded from mostwiedzy.pl

group[21]. For this purpose, three [BF_4]- bearing ionic liquids with different chain length in the imidazolium cation, that were - 1-ethyl-3-methylimidazolium tetrafluoroborate [EMIM][BF_4], [BMIM][BF_4] and 3-methyl-1-octyimidazolium tetrafluoroborate [OMIM][BF_4] were applied. We found that ionic liquids served both as a source of fluorine ions as well as a source of nitrogen and boron elements incorporated into the TiO_2 tubular structure. The electrolyte containing IL with the longest alkyl chain length in the imidazolium cation [OMIM] [BF_4] turned out to be more promising reaction medium compared to previously used electrolytes based on [BMIM][BF_4], since provided longer and wider NTs[21]. The results revealed higher efficiency of NTs formed in the ILs-contained electrolytes in comparison with conventional ethylene glycol-based one.

Since discovered that the NTs play an important role in the photocatalytic decomposition of organic pollution and could be used as a self-cleaning and anti-fogging materials, the wettability studies of NTs surface have attracted interest[27]. It is known that the wettability properties of TiO_2 NTs strongly depend on preparation methods of samples. It was observed that different annealing temperature of TiO_2 NTs (200, 400, 600 and 800°C), UV irradiation (240 min) or storing conditions and time resulted in significant changes in wettability's surface of NTs. For example, UV irradiation resulted in increased hydrophilicity of the samples (especially that annealed in 400°C) with the contact angle reduction of 90.4%[28–30]. This phenomenon was related with a presence of organic impurities in the air and aging the NTs surface[30].

Based on our previous research on the preparation of TiO_2 microspheres *via* ionic liquid assisted solvothermal method, [EAN][NO_3] was chosen as a structural agent promoting preparation of photocatalyst with an extremely high photocatalytic activity under visible irradiation. Therefore, in this study we aimed to assess the effect of this IL on the structure, surface and photocatalytic activity of TiO_2 NTs prepared by electrochemical way. In this regard, we present, for the first time, a new route to prepare photoactive ionic liquid nanotubes (IL_NTs), where

MOST WIEDZY Downloaded from mostwiedzy.pl

addition of small amount of ethylammonium nitrate [EAN][NO_3] to the traditional electrolyte (based on ethylene glycol, water and ammonium fluoride as a source of fluoride ions) play a critical role in the morphology and photocatalytic performance. We investigated the effect of various content of IL on the properties of electrolyte (dynamic viscosity, density, conductivity and surface tension) used for anodic oxidation of titanium substrate and finally how it affects morphology, wettability, structural and photocatalytic properties of NT layers.

EXPERIMENTAL SECTION

Materials

Ionic liquid ethyloammonium nitrate [EAN][NO_3] with purity ≥ 99% were purchased from Iolitec, Germany. Titania NTs arrays were obtained by anodization of titanium foil (0,127 mm thickness, 99.7% purity, Sigma Aldrich). To clean the surface of Ti foil isopropanol (p.a., POCh. S.A., Poland), acetone, methanol (p.a., P.P.H. STANLAB, Poland) and deionized water (Hydrolab BASIC 5, Poland) were used. The NTs were anodized in electrolyte composed of EG (analytical grade, CHEMPUR., Poland), ammonium fluoride (ACROS ORGANICAS), deionized water, and ionic liquid. Phenol as well as terephthalic acid (99.5%, p.a., Sigma Aldrich) were used for the photoactivity investigations.

Preparation of TiO_2 nanotubes

Titanium foil (2 x 3 cm) was ultrasonically washed in acetone, isopropanol, methanol and deionized water for 10 min each solvent and then dried in air stream before use. During the electrochemical synthesis three kind of electrodes were used, namely Ti foil as a working electrode, Pt mesh as a counter electrode and Ag/AgCl as a reference electrode. Anodization was carried out in the electrolyte composed of ethylene glycol (98% v/v), ammonium fluoride (0.2 M NH_4F), deionized water (2% v/v) and [EAN][NO_3] (0.05, 0.1, 0.2, 0.3, 0.5 and 1.0 wt.%) for 1 h at the voltage of 40 V. After preparation amorphous NTs were flushed by deionized water, dried at room temperature for 24 h, sonicated in deionized water for 5 min, dried in air

MOST WIEDZY Downloaded from mostwiedzy.pl

at 80℃ for 24 h and calcinated in the air ambience at 450℃ for 1 h.

Physicochemical properties of electrolytes

Dynamic viscosity of the electrolytes used for NTs preparation was measured by the cone and plate viscometer (LVDV – III, Brookfield Engineering Laboratory, USA) using a CP40 spindle. Density measurements were carried out using DM40 LiquiPhysics™ density meter, Mettler Toledo, USA. Conductivity measurements were performed with CX - 70 conductivity meter, Elmerton, Poland. Pendant drop method was used to determine the surface tension of electrolytes by using OCA 15 apparatus, Dataphysics, Germany. The temperature of all measurements was set at a constant level of 25 ± 0.1℃.

Surface characterization techniques of nanotubes

High resolution scanning electron microscopy (HRSEM, JEOL, JSM – 7610F) was used to determine the morphology of NTs. Based on the simple geometrical model, developed surface area of the nanotube arrays has been calculated by the following equation[31–33]:

$$S_t = \frac{8\pi h R_2}{\sqrt{3}(4R_2 - 2R_1 + y)^2} \cdot S_{geo} \quad (2)$$

where, R_1 and R_2 are the inertial radius and the sum of R_1 and half of the wall thickness, respectively, y responds to the thickness void between the nanotubes, h is the length of NTs and S_{geo} is a geometric area. Wettability changes of NTs layers by water were investigated by contact angle measurement using contour analysis system of OCA 15 goniometr, Dataphysis, Germany. The crystalline structures of TiO_2 was confirmed by X-ray diffractometer Rigaku MiniFlex 600 equipped in Cu Kα radiation, in the range of 2θ =20 - 80°. Optical properties were measured by Diffuse reflectance UV-Vis spectroscopy (Thermo Scientific) using $BaSO_4$ as a reference sample. The absorption spectra were collected in the wavelength range of 300 - 800 nm. The photoluminescence experiments were performed by a photoluminescence spectrometer LS - 50B (Perkin Elmer). The samples of NTs were excited by irradiation wavelength of 300 nm issued by Xenon lamp. X-ray photoelectron spectroscopy (XPS) experiments were performed

MOST WIEDZY Downloaded from mostwiedzy.pl

by using the PHI 500 VersaProbe (ULVAC - PHI) spectrometer with monochromatic Al Kα radiation (hν = 1486.6 eV).

Photocatalytic experiments

Photocatalytic activity of IL_NTs was measured by the degradation of phenol, used as a model contaminant of an aqueous phase. The process was carried out with a 1000 W Xenon lamp (Oriel 66021) under magnetic stirring (500 rpm). The samples of IL_NTs were placed in a quartz reactor filled with phenol solution (20 mg/L, 8 ml). The reactor was kept without light for 30 minutes and then the suspension was irradiated for 60 minutes by UV-Vis light (λ > 350 nm). During irradiation the phenol samples (0.5 ml) were collected and analysed every 20 minutes. Irradiation intensity was measured by an optical power meter (HAMAMATSU, C9536-01) and equalled to 50 mW/cm^2. The effectiveness of phenol degradation was determined by high performance liquid chromatography (HPLC, Shimadzu) using the SPD - M20A diode array detector operated at 225 nm. The flow rate of a mobile phase, composed of acetonitrile (LiChrosolv, Germany) and formic acid (Honeywell, Germany) (v/v: 20/80), was maintained at 0.3 ml/min, a sample injection volume was 20 μl.

RESULTS AND DISCUSSION

Physicochemical properties of electrolytes

The physicochemical properties of the electrolytes, used for titanium dioxide IL_NTs formation, composed of EG, H_2O, NH_4F and different amount of [EAN][NO_3] (0.05, 0.1, 0.2, 0.3, 0.5 and 1.0 wt.%), were determined by means of viscosity, density, conductivity and surface tension measurements (results are given in Table 1). It was expected that especially viscosity and conductivity of the electrolytes could play a significant role in ions movement to the TiO_2 layers. The dynamic viscosity of the electrolyte containing beside water also the lowest amount of IL, that is 0.05 wt.%, was higher in comparison to the reference one. It was due to the higher dynamic viscosity of pure ionic liquid. However, an interesting behaviour was

MOST WIEDZY Downloaded from mostwiedzy.pl

detected when the IL's content was further increased since the dynamic viscosity of the electrolyte slightly decreased from 16.33 to 16.05 mPa·s for the electrolytes containing 0.05 wt.% and 1.0 wt.% of [EAN][NO_3], respectively. This phenomenon may be explained by the weakening of the cation-anion, cation-cation and anion-anion interactions in [EAN][NO_3] due to the formation predominantly the strong interactions between nitrate and glycol[34] resulting in moving apart cation and anion. The lower viscosity means higher conductivity of the system and facilitated diffusion of reagents to the pore tips[35]. Since ILs, are salts characterised by relatively high conductivity, a modification of the electrolyte composition by addition of [EAN][NO_3] provided environment with conductivity ranging from 93.21 as detected for the sample with the lowest IL content to 151.25 $S \cdot m^{-1}$ for the sample with the highest IL content. According to the literature a higher conductivity of the anodizing solution can result in an increased of TiO_2 NTs length and cause formation a tabular structure of NTs[36], what is required from the photocatalytic point of view. For example, Kim *et al*. revealed that lower conductivity resulted in a slow growth of TiO_2 NTs and formation a fiber-like structure[36]. Addition of [EAN][NO_3] influenced also on the surface tension of the electrolytes by decreasing this parameter from 46.47 to 38.52 $mN \cdot m^{-1}$ with increasing the IL content. Dissolution of the ionic liquid in the electrolyte caused the weakening of the electrostatic and Van deer Waals interactions between the ions presented in the electrolytes resulting not only in decrease of viscosity but also surface tension. The presence of IL in the electrolytes does not affect its density.

Table 1. Physicochemical properties of electrolytes containing [EAN][NO_3] used for NTs preparation. For comparison properties of the electrolyte without IL was also given.

	Electrolyte composition	**Dynamic viscosity (mPa·s)**	**Density ($kg \cdot dm^{-3}$)**	**Conductivity ($S \cdot m^{-1}$)**	**Surface tension ($mN \cdot m^{-1}$)**
Electrolyte without IL	EG, 2% H_20, 0.2M F^-	16.12 ±0.34	0.9979 ± 0.0001	87.03 ± 0.06	47.05 ± 0.03
ILs-based electrolytes	EG, 2% H_20, 0.2M F^-, 0.05 wt.% [EAN][NO_3]	16.33 ± 0.13	0.9979 ± 0.0001	93.21 ± 0.89	46.47 ± 0.07
	EG, 2% H_20, 0.2M F^-, 0.1 wt.% [EAN][NO_3]	16.13 ± 0.29	0.9979 ± 0.0001	99.18 ± 1.12	45.81 ± 0.22

MOST WIEDZY Downloaded from mostwiedzy.pl

	EG, 2% H_20, 0.2M F^-, 0.2 wt.% [EAN][NO_3]	16.14 ± 0.21	0.9979 ± 0.0001	103.02 ± 1.23	44.49 ± 0.28
	EG, 2% H_20, 0.2M F^-, 0.3 wt.% [EAN][NO_3]	16.07 ± 0.35	0.9980 ± 0.0001	111.49 ± 0.87	42.83 ± 0.20
	EG, 2% H_20, 0.2M F^-, 0.5 wt.% [EAN][NO_3]	16.06 ± 0.20	0.9981 ± 0.0001	126.02 ± 0.91	41.63 ± 0.37
	EG, 2% H_20, 0.2M F^-, 1.0 wt.% [EAN][NO_3]	16.05 ± 0.15	0.9986 ± 0.0002	151.29 ± 0.74	38.52 ± 0.17

A typical result of current density registered during electrochemical oxidation of Ti foil at 40 V is shown in Fig. 1. A characteristic three stages of the NTs growth taking part in an electrolyte containing fluoride ions were observed. First of all (during the initial anodization time ~ 5 s), a dramatical decrease of the current density was detected reflecting formation of a dense layer of TiO_2 on the Ti foil. The next step involved activation of the barrier oxide layer by fluoride ions resulting in TiO_2 dissolution and formation of the soluble complex, according to the following equation:

$$TiO_2 + 6F^- + 4H^+ \rightarrow TiF_6^{2-} + 2H_2 \quad (1)$$

As a result of the electric field, fluoride ions can migrate deeply into the produced layer of TiO_2 causing its local digestion. This stage resulted in a slight increase of the current density (~15 s), which causes the deepening of the pores, which in time branch out. However, for electrolytes containing 0.5 and 1.0 wt.% [EAN][NO_3] we observed a strong increase of current density, around 200 s, during anodic oxidation. Due to higher conductivity of those electrolytes, which increase with increasing amount of IL, the second stage of the nanotubes formation was significantly strengthened and elongated. As mentioned above, the electrolytes conductivity substantially accelerates the process of the nanotubes growth[36]. Maintaining the optimal conditions of anodization, the current is evenly distributed between the pores, which leads to self-ordering of the porous structure that begins to resemble into the shape of the NTs. Subsequently, the processes were characterized by stabilization of the current. A further deepening of the pores with the simultaneous creation of empty spaces between them, resulted in the formation of NTs separated from each other. During the final stage of the process the

MOST WIEDZY Downloaded from mostwiedzy.pl

length of the NTs increases until to the end of the anodization.

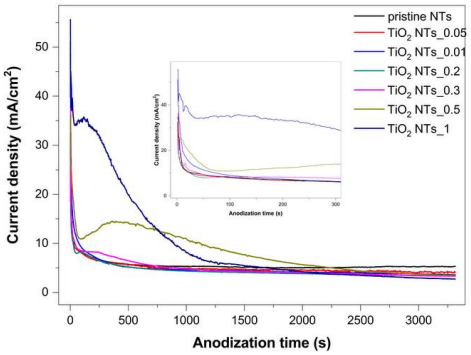

Figure 1. Current density curves recorded during anodization at 40 V for pristine and IL_NTs.

Structure of nanotubes

To determine the surface structures of the obtained samples, HRSEM images have been executed. Top view, cross-sectional and the outer wall images of pristine and IL_NTs are presented in Fig. 2. It is evident that on the all examined area vertically and regularly ordered structures of NTs were observed. Both pristine and IL_NTs were open at the top parts (see left column in Fig. 2). Despite the low water content in the electrolytes, the oxide ripples on the tube walls were noticed (see Fig. 2, right column). We suspect that the addition of IL to the electrolytes during anodization lead to specific chemical effects, such as the surface adsorption or the creation of decomposition products creation and resulted in the ripples formation. As expected, the outer diameter, wall thickness and length of the obtained photocatalysts were found to be proportionally related with increasing amount of IL content used during the anodization of Ti substrate in the electrolytes. The length of IL_NTs were elongated, starting approximately from 6.0 μm (TiO_2 NTs_0.05) and reaching approximately to 8.1 μm (TiO_2 NTs_1.0) as presented in Fig. 2. At the same time, the outer diameter and the wall thickness also changed from 107 ± 5.1 to 140 ± 4.2 nm and 5.4 ± 0.7 to 15.0 ± 1.2 nm, respectively (all dimensions have been summarized in Table 2).

We observed that the developed surface area for TiO_2 NTs_0.05 in compare with pristine TiO_2

MOST WIEDZY Downloaded from mostwiedzy.pl

NTs sample was slight higher, 1343 and 1294 cm^2 respectively. However, further increase of IL content caused an opposite effect, despite of increasing the morphological parameters of NTs. The results of the calculation for all the samples are presented in Table 2.

Crystal structure

The XRD patterns of pristine and IL_NTs are presented in Fig. 3. The diffraction peak of pristine NTs observed at 2θ of 25.51° can be assigned to crystallographic form of anatase TiO_2 (101). It was used to appointment at half the maximum intensity of the (101) reflection and based on the Scherrer equation the average crystallite size of NTs was estimated. The other peaks, observed at 2θ values of 36.93°, 37.87°, 47.88° and 54.01°, are also assigned to TiO_2, specifically (103), (004), (200) and (105), are characteristic for anatase phase. The peaks detected at 35.04°, 38.39°, 40.29°, 53.08°, 63.07°, 70.74°, 76.35°, 77.37° and 82.34° originated from the Ti foil substrate. Addition of [EAN][NO_3], up to content 0.2 wt.%, stimulated increase of the intensity of the peaks assigned to the crystal structure of anatase (101). However, further increase of the IL caused an opposite effect. The XRD parameters of NTs such as cell volumes and crystallite sizes were collected in Table 2. The results do not reveal the relation between the increasing amount of IL used for NTs synthesis, the crystallite size and the dimensional parameters of NTs.

MOST WIEDZY Downloaded from mostwiedzy.pl

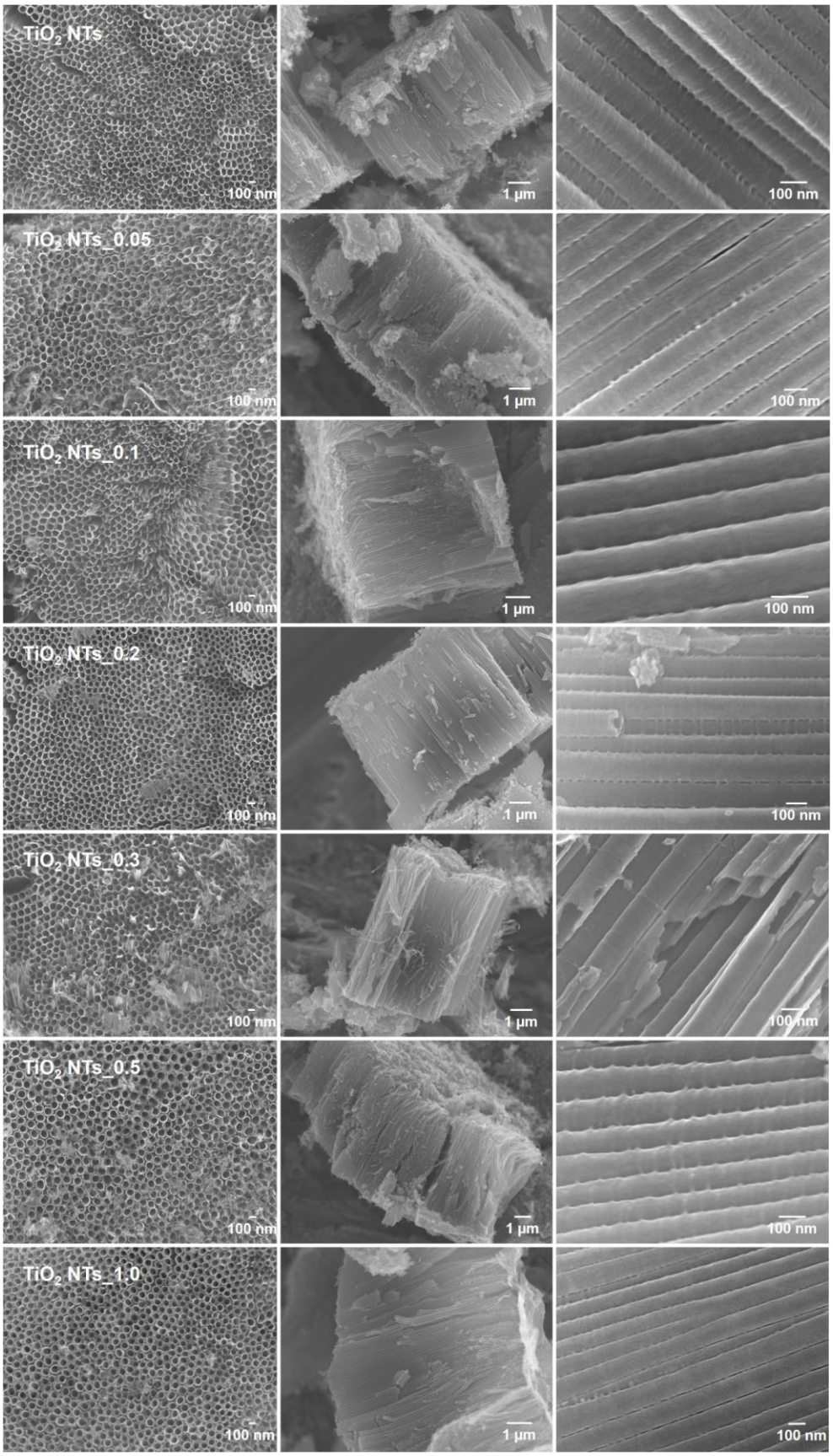

Figure 2. Surface (left column), cross-sectional (middle column), and the outer wall (right column) SEM images of IL_NTs and pristine TiO_2 NTs.

MOST WIEDZY Downloaded from mostwiedzy.pl

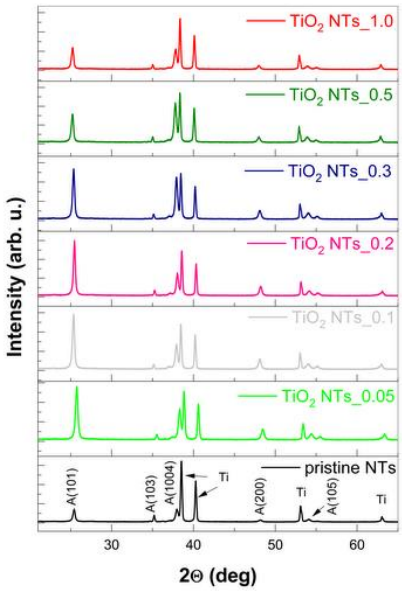

Figure 3. XRD patterns of NTs after anodization at 40 V in the electrolyte composed of EG, H_2O, NH_4F and different amount of IL.

Optical and photoluminescence properties

Photoabsorption properties of TiO_2 NTs were measured by diffuse refraction UV-Vis spectroscopy and the spectra were collected in the range of 300 – 700 nm as shown in Fig. 4a. The absorption edge of all the samples was particularly located at λ = 380 nm, which corresponds to the intrinsic band gap absorption of TiO_2 anatase (3.2 eV). Note the broad absorption band from 400 to 800 nm for all TiO_2 NTs samples, which might be associated with trapped electrons at Ti^{3+} centre, highlighting the maxima at 537.5 nm (for pristine TiO_2 NTs, TiO_2 NTs_0.05 and TiO_2 NTs_0.1), 519 nm (for TiO_2 NTs_0.2 and TiO_2 NTs_0.5), 467 nm (TiO_2 NTs_0.3) and 626 nm (TiO_2 NTs_1.0).

Photoluminescence spectra of obtained samples (PL) were registered in the range of 300 – 700 nm and excited at 300 nm, as presented in Fig. 4b. The intensity and shape of PL spectrum suggested that the TiO_2 NTs have surface defects. The spectral bands of synthesized NTs at 380 nm were ascribed to self-trapped of excitons localized on TiO_6 octahedra. Serpone *et al.*[37] described the PL spectral bands of TiO_2 anatase crystals with the wavelength at 420, 450 and

MOST WIEDZY Downloaded from mostwiedzy.pl

470 nm are attributed to oxygen vacancies. The peak at 520 nm was assigned to the radiative recombination of mobile electrons with trapped holes. Furthermore, we observed that PL intensity of TiO_2 NTs increase with changing amount of IL, the lowest was for TiO_2 NTs_0.05 and the highest was for TiO_2 NTs_1.0. It may suggest that the TiO_2 NTs_0.05 sample a better separation of photogenerated charge carries occur and thus lower recombination – lower photoluminescence intensity.

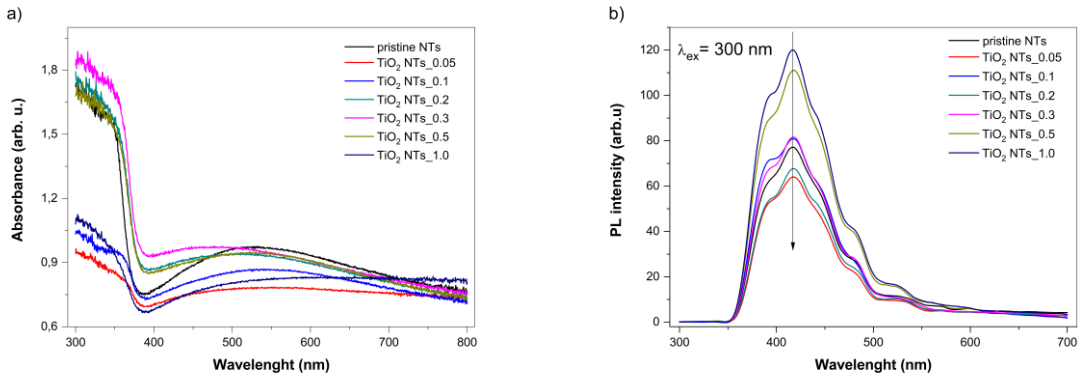

Figure 4. (a) The photoabsorption spectra of pristine and IL_NT samples recorded in the range of 300 to 800 nm, (b) PL spectra of pristine and IL_NTs with extinction wave at 300 nm in the range of 300 to 700 nm.

Chemical composition

The elemental surface composition of pristine and IL_NTs specimens, evaluated by XPS, are shown in Table S1. The titanium, oxygen, carbon, nitrogen and fluorine were detected and the corresponding high-resolution (HR) XPS spectra of Ti 2p, O 1s, C 1s and F 1s are collected in Fig. 5. The presence of carbon and nitrogen atoms, especially a C-N and C-C species (286.1 and 284.8 eV) confirm adsorption of [EAN][NO_3] at the TiO_2 surface. The chemical character of titanium, oxygen and carbon is identified in the deconvoluted spectra and summarized in Table S1. The N 1s spectra exhibited only one signal at 400 eV, assigned to the surface C-N bond. The presence of fluorine species is evidenced by the F 1s spectra (signal at 684.5 eV) and C 1s spectra (signals at 289.1 eV and 290.8 eV ascribed to CH-F and C-Fx species, respectively[38]). No correlations were observed between the fluorine surface content and the

MOST WIEDZY Downloaded from mostwiedzy.pl

Table 2. Sample label, NTs dimension and crystallographic properties of pristine and IL_NTs.

Sample label	Amount of IL (wt.%)	NTs dimensions			Developed surface area (cm^2)	XRD			
		External diameter (nm)	Tubes length (µm)	Wall thickness (nm)		Crystallite size (nm)	Cell parameters (A)		Cell volume (A^3)
							a=b	c	
pristine NTs	not used	105 ± 3.7	5.5 ± 0.21	4.4 ± 0.5	1294	29.4	3.7703(0)	9.4783(6)	134.7364(2)
TiO_2 NTs_0.05	0.05	107 ± 5.1	6.0 ± 0.15	5.4 ± 0.7	1343	25.9	3.7492(3)	9.4132(3)	132.3191(9)
TiO_2 NTs_0.1	0.1	114 ± 4.3	6.2 ± 0.17	9.4 ± 1.9	1163	33.7	3.7809(9)	9.4834(3)	135.5740(3)
TiO_2 NTs_0.2	0.2	115 ± 4.6	6.2 ± 0.18	10.0 ± 1.3	1135	37.1	3.7690(9)	9.4723(5)	134.5645(8)
TiO_2 NTs_0.3	0.3	119 ± 2.1	6.8 ± 0.20	11.0 ± 1.0	1181	29.3	3.7842(0)	9.5146(0)	136.2513(6)
TiO_2 NTs_0.5	0.5	133 ± 2.8	7.2 ± 0.24	13.0 ± 0.5	1099	32.5	3.7869(3)	9.5067(4)	136.4635(4)
TiO_2 NTs_1.0	1.0	140 ± 4.2	8.1 ± 0.20	15.0 ± 1.2	1139	31.9	3.7869(3)	9.5019(1)	134.7364(2)

MOST WIEDZY Downloaded from mostwiedzy.pl

volume of IL increasing from 0.05 up to 0.3 wt.% (Table S1). The fluorine content (0.26 ± 0.03 at.%) was found to be close to that detected for pristine NTs sample (0.29 at.%). However for samples TiO_2 NTs_0.5 and TiO_2 NTs_1.0 we observed a significant increase of fluorine amount (0.40 and 0.48 at.%, respectively). The surface amount of nitrogen increased after addition of [EAN][NO_3] up to 0.3 wt.% (Table S1). However, further increase of the IL (0.5 and 1.0%) caused systematic decrease of nitrogen contribution (0.58 and 0.38 at.%, respectively).

It should be also noted that the chemical character of titanium species seems to be not affected by IL. The relative contribution of Ti^{3+} surface species were found to be very close to pristine NTs (3.45 ± 0.14%, Table S1) for all samples, except the TiO_2 NTs_1.0. For the last sample we detected slightly larger amount of Ti^{3+} species (4.01%) contributed the titanium fraction of surface elements.

Wetting properties

Wettability properties of TiO_2 NTs prepared in the presence of [EAN][NO_3] were determined as a time-dependent change of samples in storing conditions (see Table 3). Ten-microliter droplets were used to defined measurements of the water contact angle (WCA). As a reference sample pristine TiO_2 NT layers was used, with the WCA at value 15.3 ± 1°. By increasing the IL content in the electrolyte composition, from 0.05 to 1.0 wt.% of [EAN][NO_3], the WCA increases from 9.3 ± 1° to 13.1 ± 1°, respectively. The effect of aging of TiO_2 NTs surface was examined 3 and 7 weeks after fabrication. It was found that the surface wettability's changed. IL_NTs samples showed a hydrophilic behaviour immediately after the annealing. However, storage in air caused the surface of pristine and IL_NTs gradually converted into hydrophobic. According to the literature, [EAN][NO_3] have hydrophilic character (despite presence of ethyl substituent) - is miscible with water at any composition since both ions are able to form hydrogen bonds with water[39]. Therefore, this ability of IL adsorbed on the nanotubes surface

MOST WIEDZY Downloaded from mostwiedzy.pl

facilitated spreading of water, thus caused a decrease in the WCA values of all IL_NTs samples in comparison with pristine TiO_2 NTs. Especially, the hydrophilicity of TiO_2 NTs_0.05 and TiO_2 NTs_0.1 samples was found to be higher (the WCA values were 9.3 and 9.7°, respectively) in compare to pristine TiO_2 NTs (WCA = 15.3°). In the case of the photocatalysts prepared in a presence of higher IL content probably the influence of the short hydrocarbon chain in the [EAN][NO_3] cation started to be detectable. Therefore, WCA was observed to be higher. In addition, it is well known that the absorption of the water molecules on the TiO_2 NT layers is facilitated due to the presence of the oxygen vacancies at the surface what allowing faster spread of the water droplets [40,41]. Therefore, the WCA is always lower at the surface with higher content of oxygen vacancies. Based on the XPS analysis, we observed that samples obtained in the presence of [EAN][NO_3] contained higher amount of hydroxyl groups in compare to pristine TiO_2 NTs which could be attributed to the ability to hydrogen bonding to hydroxyl groups. The hydrophilicity of all IL_NTs samples is higher than pristine TiO_2 NTs also due to higher amount of hydroxyl groups at the surface, respectively 2.26 and 2.42 for TiO_2 NTs_0.05 and TiO_2 NTs_0.1 and for pristine TiO_2 NTs – 1.58%. According to the literature, the existence of OH groups is related with adsorption and dissociation of water molecules on the surface of TiO_2 nanotubes[42–44]. The loss of the hydrophilicity in the atmosphere of air is the reason for the adsorption of foreign compounds on the clean surface of TiO_2 NTs, such as water and volatile organic compounds (VOC). Variation of a water drop shape at the analysed NTs and IL_NTs surface is shown in Table 3. Differences in WCA might be also attributed to the surface properties, especially the surface roughness, which in our case, increase with increasing amount of [EAN][NO_3] used as the addition to the electrolytes during the anodization.

MOST WIEDZY Downloaded from mostwiedzy.pl

Table 3. Comparison of the time-dependent change of TiO_2 NTs surface wettability.

Sample label	Water contact angle (°)		
	0 days*	21 days*	49 days*
pristine NTs	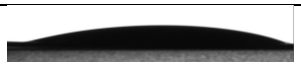 WCA = 15.3 ± 1°	 WCA = 17.8 ± 2°	 WCA = 19.7 ± 2°
TiO_2 NTs_0.05	 WCA = 9.3 ± 1°	 WCA = 11.0 ± 2°	 WCA = 19.7 ± 2°
TiO_2 NTs_0.1	 WCA = 9.72 ± 1°	 WCA = 14.4 ± 1°	 WCA = 23.4 ± 2°
TiO_2 NTs_0.2	 WCA =10.2 ± 1°	 WCA = 22.5 ± 1°	 WCA = 26.4 ± 1°
TiO_2 NTs_0.3	 WCA = 10.45 ± 1°	 WCA = 25.1 ± 3°	 WCA = 28.3 ± 2°
TiO_2 NTs_0.5	 WCA = 12.43 ± 1°	 WCA = 27.3 ± 2°	 WCA = 39.3 ± 2°
TiO_2 NTs_1.0	 WCA = 13.1 ± 1°	 WCA = 43.67 ± 2°	 WCA = 51.5 ± 2°

* time measured from the preparation of samples

Moreover, TiO_2 NTs_0.05 was the sample, which exhibited the highest hydrophilic properties with the lowest tube diameter (107 nm). The highest change in WCA for TiO_2 NTs_0.5 and TiO_2 NTs_1.0 were observed, both after preparation and storage in the air ambiance for 3 and 7 weeks (see Fig. S1). This phenomenon could be attributed to the increase of the wall thickness of NTs with increasing amount of IL. Higher thickness of the walls may impede penetration of the IL_NTs surface by the water droplets. According to the literature, modification of the NTs by organic compounds, significantly change the wettability. Balaur *et al.*[5] observed the relation

MOST WIEDZY Downloaded from mostwiedzy.pl

between chemical character of solvents, organic and non-organic, as well as the tube diameter and the properties of the wetted surfaces. The water contact angle changed with increasing diameter of NTs from 134 ± 3° for the 20 nm pores to 159 ± 2° for the 100 nm pores, respectively. The opposite effect was observed for organic solvent, hexadecane. By increasing the diameter of NTs contact angle changed from 21 ± 2° for the 20 nm pores and became super hydrophilic θ ~ 0° for the 100 nm pores.

Photocatalytic properties

The results of phenol degradation rate under UV-Vis irradiation are presented in Fig. 6a and Table 4. To visualize the real photocatalytic properties of as-prepared samples, control test (photolysis) has been performed. Approximately 10% of phenol loss was observed with the absence of photocatalysts under UV-Vis irradiation and it indicates that photocatalytic activity comes from prepared samples. Evidently, we found much higher values of phenol degradation in the presence of samples prepared with addition of ILs with respect to pristine NTs. The sample with the highest photoactivity, TiO_2 NTs_0.05, was characterized by initial reaction rate at the level of 9.12 $\mu mol \cdot min^{-1} \cdot dm^{-3}$ (85% efficient of phenol degradation after 20 min of UV-Vis irradiation). In comparison to pristine NTs, the reaction rate of TiO_2 NTs_0.05 was approximately two times higher. It suggested that addition of the smallest amount of [EAN][NO_3] significantly changed photoactivity of NTs. Decomposition of phenol in the reaction mixture was relatively fast, for samples TiO_2 NTs_0.05, TiO_2 NTs_0.1, TiO_2 NTs_0.2 and TiO_2 NTs_0.3 phenol was not determinable after 40 minutes of irradiation. By increase of the IL content the photocatalytic activity of IL_NTs under UV-Vis irradiation decreases: the lowest photocatalytic activity was observed for TiO_2 NTs_1.0. The values of TiO_2 NTs_1.0 changed from 7.10 to 3.51 $\mu mol \cdot dm^{-3} \cdot min^{-1}$, namely degradation efficiently reached 95.76% after 40 min of UV irradiation.

MOST WIEDZY Downloaded from mostwiedzy.pl

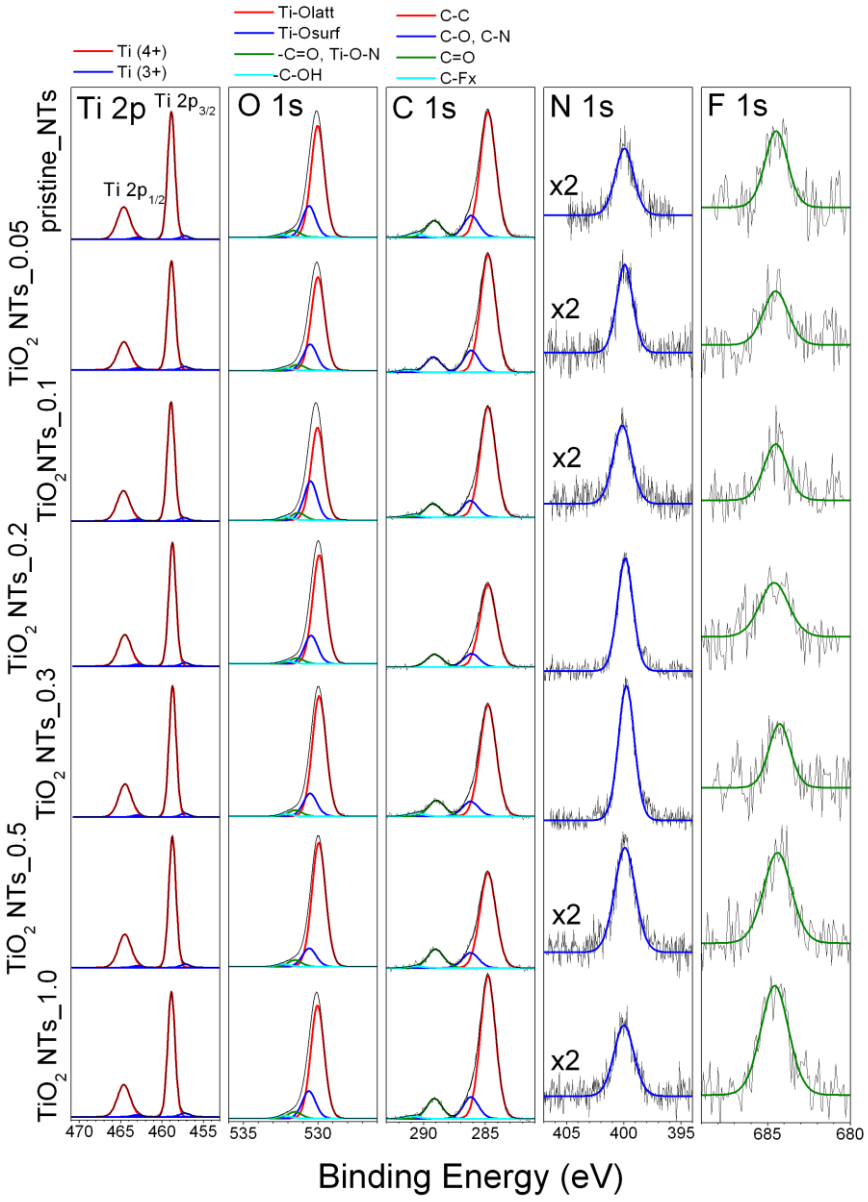

Figure 5. High resolution XPS spectra of Ti 2p, O 1s, C 1s, N 1s and F 1s recorded on pristine and IL_NTs. The chemical character of detected elements is described in deconvoluted spectra.

The sample TiO_2 NTs_0.5 showed slightly lower ability to degrade phenol, in comparison with TiO_2 NTs_0.05, the values equalled at 83% (with initial reaction rate 8.59 µmol·dm^{-3}·min^{-1}) for TiO_2 NTs_0.5 and 85% (9.12 µmol·dm^{-3}·min^{-1}) for TiO_2 NTs_0.05, respectively. However, this was the sample, which exhibited the highest ability to generate •OH, more than three times in comparison with TiO_2 NTs_0.05, as shown in Fig. 6b. This suggests that also $O_2^{\bullet-}$ radicals play a vital role in the process of phenol degradation under UV-Vis light. A correlation between

MOST WIEDZY Downloaded from mostwiedzy.pl

efficiency of phenol degradation and generation of •OH was not observed.

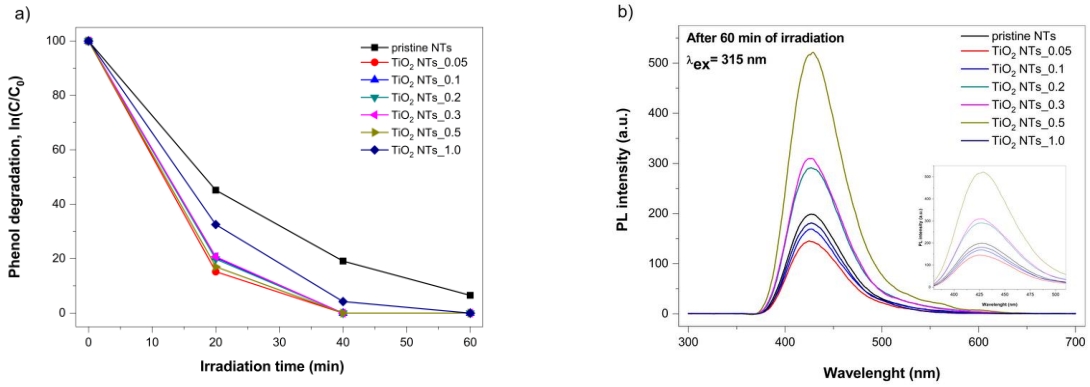

Figure 6. (a) Phenol degradation and (b) generation of hydroxyl radical under UV-Vis irradiation.

Phenol degradation measurements in the presence of NTs under UV-Vis irradiation led to detect intermediate forms of phenol at wavelength 254 nm, such as benzoquinone, resorcinol, catechol and hydroquinone. During photodegradation process concentration of by-products were decreasing to values 0 µmol·dm^{-3} after 60 minutes to all IL_NTs samples (see Table 3), which suggested high phenol mineralization to CO_2 and H_2O.

The most representative and photoactive sample, TiO_2 NTs_0.05, was chosen to define the formation of reactive oxygen species (ROS) during a process of phenol degradation. Selected scavengers, namely silver nitrate, *tert*-butanol, oxalic acid and benzoquinone were used as scavengers of e^-, $\bullet OH$, h^+ and $O_2^{\bullet -}$, respectively (see Fig. 7a). The photocatalytic efficiency of phenol degradation in the presence of benzoquinone and oxalic acid reached 81 and 82%, respectively, whereas addition of *tert*-butanol and silver nitrate caused decrease in the photocatalytic efficiency at level 7 and 2% respectively. It suggested that the e^- and h^+ have the greatest significance during phenol degradation and allow oxidation and reduction reaction occurred.

The photostability of the most photoactive sample (TiO_2 NTs_0.05) was investigated by reaction of phenol degradation in four consecutive cycles, and the results are collated in Fig 7b. Phenol degradation rate remained at the level 3.38 µm·dm^{-3}·mol^{-1} for the first two cycles,

MOST WIEDZY Downloaded from mostwiedzy.pl

3.36 μmol·dm^{-3}·min^{-1} for third one and for the last cycle 3.41 μmol·dm^{-3}·min^{-1} after 60 minutes of UV-Vis irradiation. It clearly suggested high photostability of the obtained NTs.

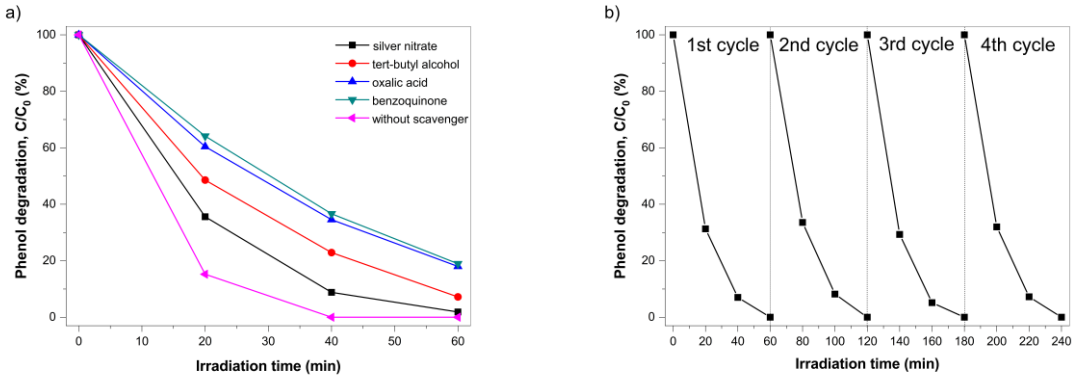

Figure 7. (a) Photocatalytic decomposition of phenol under UV-Vis irradiation in the present of scavengers (silver nitrate, *tert*-butyl alcohol, oxalic acid and benzoquinone), (b) photostability of the most photoactive sample (TiO_2 NTs_0.05) in reaction of phenol degradation in four consecutive cycles under UV-Vis irradiation.

Formation and photocatalytic mechanism discussion

Based on the literature and our experience, we found that the physicochemical properties of electrolytes containing IL, such as dynamic viscosity, conductivity and surface tension, play a key role in the tubes growth process. Practical constantly values of dynamic viscosity allows to the ions movement into the dioxide layers and influence formation of the local digestion[35]. Moreover, during anodic oxidation in a presence of IL, the ions from the electrolyte enable a faster ionic conduction through the barrier layer, caused a higher nanotubes growth[36] (see Fig. 8a). We also suspect that the decrease in the surface tension with increasing amount of IL is connected with the increase of the morphological parameters (as presented in Fig. 8b).

As mentioned above, the samples obtained in the presence of IL highlighted larger morphological dimensions compared to the pristine NTs sample. The length of the NTs was in the range from 6.0 to 8.1 μm (5.5 μm for pristine NTs) and mainly the increased electrolyte conductivity and lower viscosity have contributed to this phenomenon. In the cause of low conducting organic electrolytes, as used in our study, greater conductivity of the electrolyte leads to increase of the growth rate of the nanotubes[45] as a result of reduction of Ohmic drop,

MOST WIEDZY Downloaded from mostwiedzy.pl

resistivity (iR_{cell}) and causes higher overpotential.

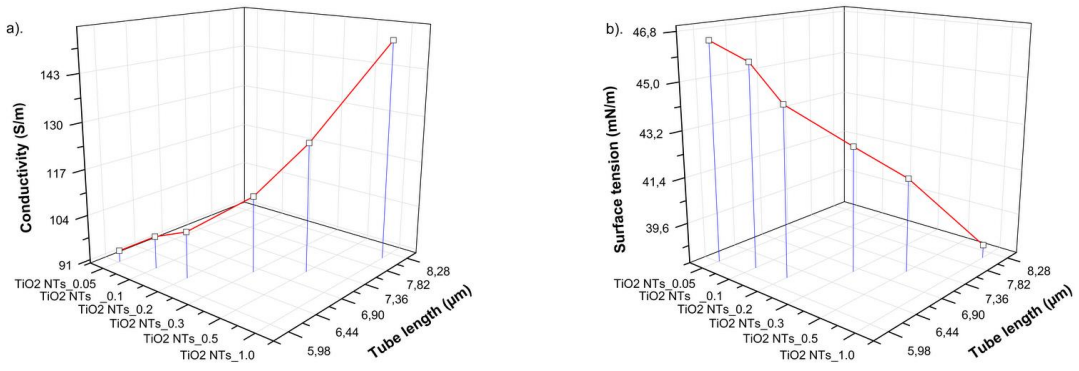

Figure 8. Influence of conductivity (a) and surface tension (b) on the tube growth process.

Similar effect has been achieved by using the same electrolyte several times, namely nanotube length increased as the number of anodization process raises[36]. Furthermore, the presence of additional non-metal elements such as C, N and F were detected in all obtained samples by XPS analysis. These elements originate from the electrolyte[46]. No appreciable increase in the carbon and fluorine content in the samples prepared from the electrolyte containing IL was observed. However, in almost all samples obtained in the presence of [EAN][NO_3], excess nitrogen amount was detected compared to the reference sample (pristine NTs), which may come from the IL decomposition during synthesis process.

MOST WIEDZY Downloaded from mostwiedzy.pl

Table 4. Initial reaction rate, reaction rate constant and by-products concentration during phenol degradation obtained for TiO_2 NTs samples in comparison to pristine TiO_2 (by products were below detection limit after 60 minutes of irradiation).

Sample label	Photocatalytic degradation of phenol		By-products concentration (µmol·dm^{-3})							
	Initial reaction rate, *r* (µmol·min^{-1}·dm^{-3})	Reaction rate constant, *k* (min^{-1})	Benzoquinone		Resorcinol		Catechol		Hydroquinone	
			20 min	40 min	20 min	40 min	20 min	40 min	20 min	40 min
pristine NTs	5.53	0.0712	2.57	4.06	3.05	3.20	23.72	38.68	26.59	14.54
TiO_2 NTs_0.05	9.12	0.0941	1.90	1.00	18.06	6.82	15.86	11.51	49.38	38.44
TiO_2 NTs_0.1	8.35	0.0794	1.53	0.88	6.70	2.12	9.01	5.93	42.03	24.26
TiO_2 NTs_0.2	8.45	0.0809	2.06	0.85	7.25	5.29	18.87	14.31	39.14	12.17
TiO_2 NTs_0.3	8.38	0.0787	3.70	0.89	9.80	5.21	16.39	15.12	36.31	21.28
TiO_2 NTs_0.5	8.59	0.0886	3.91	0.96	15.44	0	18.70	11.68	42.15	23.85
TiO_2 NTs_1.0	7.10	0.0744	5.21	1.37	15.51	0	45.61	13.89	50.59	38.87

MOST WIEDZY Downloaded from mostwiedzy.pl

To confirm the source of this additional nitrogen, the electrolyte was analysed using ion chromatography before and after the anodization process. For this study, electrolyte composed of EG, 2 vol.% H_2O, 0.2 M NH_4F and 0.05 wt.% [EAN][NO_3] was examined. Firstly, we analysed the cation of the ionic liquid and we did not find a clear difference (the difference was 1% - this is a margin of error) in the amount of cation before and after the anodization, which indicated that the IL cation does not decompose and does not give additional nitrogen to TiO_2 NTs. Thus, the anion derived from the [EAN][NO_3] was analysed. The concentration of nitrates before and after anodic oxidation was equal to 2.179 and 1.991 mg/L, respectively (results are presented in Table S2, supporting materials). This slight decrease in the nitrates content may indicate that the nitrogen in the synthesized samples originate from the anion of the used IL.

The above-mentioned two aspects (additional nitrogen and increased length) which have been achieved using [EAN][NO_3] as an additive to a traditional organic electrolyte may have a major impact on the photocatalytic properties that were significantly improved. However, if we consider the chemical structure of nitrogen then it turns out that the N 1s spectra presents one signal at 400 eV which can be attributed to surface C-N bond, associated rather with the adsorption of this element on the surface than with doping. Similar peak at 400 eV was also detected in commercial TiO_2 photocatalysts (such as ST01, Ishihara Sangyo)[47]. In addition, it has been found that mentioned chemical state is dependent on the preparation method and was observed in photocatalysts prepared via wet processes, namely sol−gel and hydrolysis processes[47]. Recent developments in this area of research have led to conclusion that rather nitrogen species detected at lower binding energies (396 – 398 eV) are responsible for the photocatalytic activity[47]. Thus, enhanced photocatalytic performance of NTs prepared with addition of IL is rather related to morphological dimensions than the presence of nitrogen on the surface.

Studies outlined in the literature prove that photocatalytic properties of NTs depend on the two

MOST WIEDZY Downloaded from mostwiedzy.pl

major factors: (1) tube morphology (mainly length and tube tops) on light absorption and (2) tube morphology on the phenomenon of recombination of photogenerated charge carriers (positive holes and negative electrons)[48]. The optimum tube length for photocatalytic application varied from 1 up to 17 μm[49–53], which was achieved depending on the preparation method (the anodization environment). Our current study supports previous findings, the highest reaction rate constant and initial reaction rate (0.0941 min^{-1} and 9.12 $\mu mol \cdot min^{-1} \cdot dm^{-3}$) were observed for NTs with the following dimensions: length 6.0 μm external diameter 107 nm and wall thickness 5.4 nm. Further increase of these dimensions (up to: length 8.1 μm external diameter 140 nm and wall thickness 15 nm) by applying a larger amount of ionic liquid in the electrolyte led to the weakening of the photocatalytic properties. Despite of the enhanced photocatalytic activity of IL_NTs, it is not correlated with the morphological parameters. However, it is obvious that present of [EAN][NO_3] caused increase both, the photocatalytic activity and dimensional parameters in compare with pristine NTs. Sample obtained with the largest addition of ionic liquid (TiO_2 NTs_1.0), showing the largest geometric dimensions has the lowest photocatalytic activity but still higher than pristine NTs. Moreover, the best sample (TiO_2 NTs_0.05) exhibited the highest developed surface area (1343 cm^2), low content of nitrogen impurities (0.55 at.%), the lowest crystallites' size (25.9 nm), high content of Ti^{3+} (0.95 at.%) and –OH groups (1.37 at.%) which is in line with the previous results reported in the literature and promotes high photocatalytic activity[53–55].

CONCLUSIONS

We have obtained comprehensive results revealing that an addition of IL, namely ethylammonium nitrate [EAN][NO_3] to the traditional organic electrolyte composed of NH_4F, H_2O and EG allows the formation of NTs with variable morphological parameters and strongly affect the photocatalytic activity. As expected, the addition of [EAN][NO_3] improves the electrolyte properties, primarily in terms of conductivity, which accelerates the growth rate of

MOST WIEDZY Downloaded from mostwiedzy.pl

well-organized NTs. The proposed route allowed to obtain NTs with extended diameter (from 107 up to 140 nm), wall thickness (from 5.4 to 15 nm) and length (from 6 to 8.1 μm). High hydrophilicity of all TiO_2 NT samples was observed immediately after annealing. However, storing in air caused the increase of the contact angle values due to absorption of impurities from the environment. Noteworthy differences were found in photoactivity of all IL_NTs samples in comparison to pristine TiO_2 NTs. The highest reaction constant rate and initial reaction rate (0.0941 min^{-1} and 9.12 $\mu mol \cdot min^{-1} \cdot dm^{-3}$, remained at the same level after four sequence tests) displayed the sample with the lowest amount of IL - TiO_2 NTs_0.05 as a result of better ability to light photoabsorption and limiting recombination losses. However, despite too extended geometrical dimensions, the other IL_NT samples exhibited impaired photocatalytic activity but still better compared to the pristine one. After 60 minutes of the photocatalytic reaction, no presence of the aromatic intermediates of phenol oxidation has been noted. Insightful XPS and HPLC analysis indicated that IL does not decompose during the anodization. It is likely that the appearance of C-N bond is associated with absorption of the IL at the TiO_2 surface. Therefore, our study provides the framework for a new way to prepare TiO_2 NTs possessing tunable morphology and thus effectively utilize renewable energy source to solve environmental problems using heterogeneous photocatalysis processes.

ASSOCIATED CONTENT

Supporting Information. The elemental surface composition evaluated by XPS, ions chromatography results of electrolyte, relationship between contact angle, diameter and amount of the IL.

AUTHOR INFORMATION

Corresponding Authors

J. Łuczak: E-mail: justyna.luczak@pg.gda.pl

P. Mazierski: E-mail: pawel.mazierski@phdstud.ug.edu.pl

MOST WIEDZY Downloaded from mostwiedzy.pl

Author Contributions

The manuscript was written through contributions of all authors. All authors have given approval to the final version of the manuscript.

ACKNOWLEDGEMENTS

The author P.M. acknowledges funding from the National Science Centre within program ETIUDA 5 (grant entitled: "Modified TiO_2 nanotubes: synthesis, characterization and application"), contract No. 2017/24/T/ST5/00221.

The author J.Ł. acknowledges funding from the National Science Centre within program SONATA 8 (grant entitled: "Influence of the ionic liquid structure on interactions with TiO_2 particles in ionic liquid assisted hydrothermal synthesis"), contract No. 2014/15/D/ST5/0274.

REFERENCES

(1) Kääriäinen, M.-L.; Kääriäinen, T. O.; Cameron, D. C. Titanium Dioxide Thin Films, Their Structure and Its Effect on Their Photoactivity and Photocatalytic Properties. *Thin Solid Films* **2009**, *517* (24), 6666–6670.

(2) Mor, G. K.; Shankar, K.; Paulose, M.; Varghese, O. K.; Grimes, C. A. Enhanced Photocleavage of Water Using Titania Nanotube Arrays. *Nano Lett.* **2005**, *5* (1), 191–195.

(3) Mor, G. K.; Carvalho, M. A.; Grimes, C. A. A Room-Temperature TiO 2 -Nanotube Hydrogen Sensor Able to Self-Clean Photoactively from Environmental Contamination. **2004**.

(4) Zhu, K.; Neale, N. R.; Miedaner, A.; Frank, A. J. Enhanced Charge-Collection Efficiencies and Light Scattering in Dye-Sensitized Solar Cells Using Oriented TiO2 Nanotubes Arrays. *Nano Lett.* **2007**, *7* (1), 69–74.

(5) Balaur, E.; Macak, J. M.; Tsuchiya, H.; Schmuki, P. Wetting Behaviour of Layers of TiO2 Nanotubes with Different Diameters. *J. Mater. Chem.* **2005**, *15* (42), 4488.

(6) Popat, K. C.; Eltgroth, M.; LaTempa, T. J.; Grimes, C. A.; Desai, T. A. Titania Nanotubes: A Novel Platform for Drug-Eluting Coatings for Medical Implants? *Small* **2007**, *3* (11), 1878–1881.

(7) Popat, K. C.; Leoni, L.; Grimes, C. A.; Desai, T. A. Influence of Engineered Titania Nanotubular Surfaces on Bone Cells. *Biomaterials* **2007**, *28* (21), 3188–3197.

(8) Fei Yin, Z.; Wu, L.; Gui Yang, H.; Hua Su, Y. Recent Progress in Biomedical Applications of Titanium Dioxide. *Phys. Chem. Chem. Phys.* **2013**, *15* (14), 4844.

(9) Roy, P.; Berger, S.; Schmuki, P. TiO2 Nanotubes: Synthesis and Applications. *Angew. Chemie - Int. Ed.* **2011**, *50* (13), 2904–2939.

(10) Kasuga, T.; Hiramatsu, M.; Hoson, A.; Sekino, T.; Niihara, K. Formation of Titanium

MOST WIEDZY Downloaded from mostwiedzy.pl

Oxide Nanotube. *Langmuir* **1998**, *14* (12), 3160–3163.

(11) Suzuki, Y.; Yoshikawa, S. Synthesis and Thermal Analyses of TiO2-Derived Nanotubes Prepared by the Hydrothermal Method. *J. Mater. Res.* **2004**, *19* (4), 982–985.

(12) Sander, M. S.; Côté, M. J.; Gu, W.; Kile, B. M.; Tripp, C. P. Template-Assisted Fabrication of Dense, Aligned Arrays of Titania Nanotubes with Well-Controlled Dimensions on Substrates. *Adv. Mater.* **2004**, *16* (22), 2052–2057.

(13) Paramasivam, I.; Macak, J. M.; Selvam, T.; Schmuki, P. Electrochemical Synthesis of Self-Organized TiO2 Nanotubular Structures Using an Ionic Liquid (BMIM-BF4). *Electrochim. Acta* **2008**, *54* (2), 643–648.

(14) Li, B.; Gao, X.; Zhang, H. C.; Yuan, C. Energy Modeling of Electrochemical Anodization Process of Titanium Dioxide Nanotubes. *ACS Sustain. Chem. Eng.* **2014**, *2* (3), 404–410.

(15) Sreekantan, S.; Lockman, Z.; Hazan, R.; Tasbihi, M.; Tong, L. K.; Mohamed, A. R. Influence of Electrolyte PH on TiO2 Nanotube Formation by Ti Anodization. *J. Alloys Compd.* **2009**, *485* (1–2), 478–483.

(16) Quiroz, H. P.; Quintero, F.; Arias, P. J.; Dussan, A.; Zea, H. R. Effect of Fluoride and Water Content on the Growth of TiO2 Nanotubes Synthesized via Ethylene Glycol with Voltage Changes during Anodizing Process. *J. Phys. Conf. Ser.* **2015**, *614* (1).

(17) D, G.; A, G. C.; K, V. O.; C, H. W.; S, S. R.; Z, C.; C, D. E. Titanium Oxide Nanotube Arrays Prepared by Anodic Oxidation J. Mater. *Res* **2001**, *16*, 3331–3334.

(18) Macak, J. M.; Sirotna, K.; Schmuki, P. Self-Organized Porous Titanium Oxide Prepared in Na2SO4/NaF Electrolytes. *Electrochim. Acta* **2005**, *50* (18), 3679–3684.

(19) Ochiai, T.; Fujishima, A. Photoelectrochemical Properties of TiO2 Photocatalyst and Its Applications for Environmental Purification. *J. Photochem. Photobiol. C Photochem. Rev.* **2012**, *13* (4), 247–262.

(20) Li, H.; Qu, J.; Cui, Q.; Xu, H.; Luo, H.; Chi, M.; Meisner, R. A.; Wang, W.; Dai, S. TiO2 Nanotube Arrays Grown in Ionic Liquids: High-Efficiency in Photocatalysis and Pore-Widening. *J. Mater. Chem.* **2011**, *21* (26), 9487.

(21) Mazierski, P.; Łuczak, J.; Lisowski, W.; Winiarski, M. J.; Klimczuk, T.; Zaleska-Medynska, A. The ILs-Assisted Electrochemical Synthesis of TiO2 Nanotubes: The Effect of Ionic Liquids on Morphology and Photoactivity. *Appl. Catal. B Environ.* **2017**, *214*, 100–113.

(22) Łuczak, J.; Paszkiewicz, M.; Krukowska, A.; Malankowska, A.; Zaleska-Medynska, A. Ionic Liquids for Nano- and Microstructures Preparation. Part 1: Properties and Multifunctional Role. *Adv. Colloid Interface Sci.* **2016**, *230*, 13–28.

(23) Łuczak, J.; Paszkiewicz, M.; Krukowska, A.; Malankowska, A.; Zaleska-Medynska, A. Ionic Liquids for Nano- and Microstructures Preparation. Part 2: Application in Synthesis. *Adv. Colloid Interface Sci.* **2016**, *227*, 1–52.

(24) Mazierski, P.; Łuczak, J.; Lisowski, W.; Winiarski, M. J.; Klimczuk, T.; Zaleska-Medynska, A. The ILs-Assisted Electrochemical Synthesis of TiO2 Nanotubes: The Effect of Ionic Liquids on Morphology and Photoactivity. *Appl. Catal. B Environ.* **2017**, *214*, 100–113.

(25) Li, H.; Martha, S. K.; Unocic, R. R.; Luo, H.; Dai, S.; Qu, J. High Cyclability of Ionic Liquid-Produced TiO2 Nanotube Arrays as an Anode Material for Lithium-Ion Batteries.

MOST WIEDZY Downloaded from mostwiedzy.pl

J. Power Sources **2012**, *218*, 88–92.

(26) Wender, H.; Feil, A. F.; Diaz, L. B.; Ribeiro, C. S.; Machado, G. J.; Migowski, P.; Weibel, D. E.; Dupont, J.; Teixeira, S. R. Self-Organized TiO 2 Nanotube Arrays: Synthesis by Anodization in an Ionic Liquid and Assessment of Photocatalytic Properties. *ACS Appl. Mater. Interfaces* **2011**, *3* (4), 1359–1365.

(27) Colmenares, J. C.; Nair, V.; Kuna, E.; Łomot, D. Development of Photocatalyst Coated Fluoropolymer Based Microreactor Using Ultrasound for Water Remediation. *Ultrason. Sonochem.* **2018**, *41*, 297–302.

(28) Zhang, M.; Yao, G.; Cheng, Y.; Xu, Y.; Yang, L.; Lv, J.; Shi, S.; Jiang, X.; He, G.; Wang, P.; et al. Temperature-Dependent Differences in Wettability and Photocatalysis of TiO2 Nanotube Arrays Thin Films. *Appl. Surf. Sci.* **2015**, *356*, 546–552.

(29) Yang, L.; Zhang, M.; Shi, S.; Lv, J.; Song, X.; He, G.; Sun, Z. Effect of Annealing Temperature on Wettability of TiO2 Nanotube Array Films. *Nanoscale Res. Lett.* **2014**, *9* (1), 621.

(30) Shin, D. H.; Shokuhfar, T.; Choi, C. K.; Lee, S. H.; Friedrich, C. Wettability Changes of TiO2 Nanotube Surfaces. *Nanotechnology* **2011**, *22* (31).

(31) Ngaboyamahina, E.; Cachet, H.; Pailleret, A.; Sutter, E. M. M. Photo-Assisted Electrodeposition of an Electrochemically Active Polypyrrole Layer on Anatase Type Titanium Dioxide Nanotube Arrays. *Electrochim. Acta* **2014**, *129*, 211–221.

(32) Pu, P.; Cachet, H.; Ngaboyamahina, E.; Sutter, E. M. M. Relation between Morphology and Conductivity in TiO2 Nanotube Arrays: An Electrochemical Impedance Spectrometric Investigation. *J. Solid State Electrochem.* **2013**, *17* (3), 817–828.

(33) Kontos, A. G.; Kontos, A. I.; Tsoukleris, D. S.; Likodimos, V.; Kunze, J.; Schmuki, P.; Falaras, P. Photo-Induced Effects on Self-Organized TiO2 Nanotube Arrays: The Influence of Surface Morphology. *Nanotechnology* **2009**, *20* (4).

(34) Mariani, A.; Campetella, M.; Fasolato, C.; Daniele, M.; Capitani, F.; Bencivenni, L.; Postorino, P.; Lupi, S.; Caminiti, R.; Gontrani, L. A Joint Experimental and Computational Study on Ethylammonium Nitrate-Ethylene Glycol 1:1 Mixture. Structural, Kinetic, Dynamic and Spectroscopic Properties. *J. Mol. Liq.* **2017**, *226*, 2–8.

(35) Macak, J. M.; Schmuki, P. Anodic Growth of Self-Organized Anodic TiO2nanotubes in Viscous Electrolytes. *Electrochim. Acta* **2006**, *52* (3), 1258–1264.

(36) Kim, J.; Kim, H.; Lee, Y.; Tak, Y. Effect of Electrolyte Conductivity on the Formation of a Nanotubular \ch{TiO2} Photoanode for a Dye-Sensitized Solar Cell. *J. Korean Phys. Soc.* **2009**, *54* (3), 1027–1031.

(37) Serpone, N.; Lawless, D.; Khairutdinov, R. Size Effects on the Photophysical Properties of Colloidal Anatase TiO2 Particles: Size Quantization versus Direct Transitions in This Indirect Semiconductor? *J. Phys. Chem.* **1995**, *99* (45), 16646–16654.

(38) Naumkin, A. V.; Kraut-Vass, A.; Gaarenstroom, S. W.; Powell, C. J. NIST X-ray Photoelectron Spectroscopy Database.

(39) Kanzaki, R.; Uchida, K.; Song, X.; Umebayashi, Y.; Ishiguro, S. Acidity and Basicity of Aqueous Mixtures of a Protic Ionic Liquid, Ethylammonium Nitrate. *Anal. Sci.* **2008**, *24* (10), 1347–1349.

(40) Hu, H.; Ji, H. F.; Sun, Y. The Effect of Oxygen Vacancies on Water Wettability of a ZnO Surface. *Phys. Chem. Chem. Phys.* **2013**, *15* (39), 16557–16565.

MOST WIEDZY Downloaded from mostwiedzy.pl

(41) Sarkar, T.; Ghosh, S.; Annamalai, M.; Patra, A.; Stoerzinger, K.; Lee, Y.-L.; Prakash, S.; Motapothula, M. R.; Shao-Horn, Y.; Giordano, L.; et al. The Effect of Oxygen Vacancies on Water Wettability of Transition Metal Based $SrTiO_3$ and Rare-Earth Based Lu_2O_3. *RSC Adv.* **2016**, *6* (110), 109234–109240.

(42) Dai, J.; Song, Y. First Principles Study on the Interaction Mechanisms of Water Molecules on TiO2 Nanotubes. *Materials (Basel).* **2016**, *9* (12), 1018.

(43) Rendón-Rivera, A.; Toledo-Antonio, J. A.; Cortés-Jácome, M. A.; Angeles-Chávez, C. Generation of Highly Reactive OH Groups at the Surface of TiO2nanotubes. *Catal. Today* **2011**, *166* (1), 18–24.

(44) Fujishima, A.; Zhang, X.; Tryk, D. A. TiO2 Photocatalysis and Related Surface Phenomena. *Surf. Sci. Rep.* **2008**, *63* (12), 515–582.

(45) Lee, K.; Mazare, A.; Schmuki, P. One-Dimensional Titanium Dioxide Nanomaterials: Nanotubes. *Chem. Rev.* **2014**, *114* (19), 9385–9454.

(46) Regonini, D.; Bowen, C.; Jaroenworaluck, A.; Stevens, R. A Review of Growth Mechanism, Structure and Crystallinity of Anodized TiO2 Nanotubes. *Mater. Sci. Eng. R Reports* **2013**.

(47) Asahi, R.; Morikawa, T.; Irie, H.; Ohwaki, T. Nitrogen-Doped Titanium Dioxide as Visible-Light-Sensitive Photocatalyst: Designs, Developments, and Prospects. *Chem. Rev.* **2014**, *114* (19), 9824–9852.

(48) Nischk, M.; Mazierski, P.; Gazda, M.; Zaleska-Medynska, A. Ordered TiO2 Nanotubes: The Effect of Preparation Parameters on the Photocatalytic Activity in Air Purification Process. *Appl. Catal. B Environ.* **2014**, *144*, 674–685.

(49) Liu, Z.; Zhang, X.; Nishimoto, S.; Murakami, T.; Fujishima, A. Efficient Photocatalytic Degradation of Gaseous Acetaldehyde by Highly Ordered TiO_2 Nanotube Arrays. *Environ. Sci. Technol.* **2008**, *42* (22), 8547–8551.

(50) Kontos, A. G.; Katsanaki, A.; Maggos, T.; Likodimos, V.; Ghicov, A.; Kim, D.; Kunze, J.; Vasilakos, C.; Schmuki, P.; Falaras, P. Photocatalytic Degradation of Gas Pollutants on Self-Assembled Titania Nanotubes. *Chem. Phys. Lett.* **2010**, *490* (1–3), 58–62.

(51) Mazierski, P.; Nischk, M.; Gołkowska, M.; Lisowski, W.; Gazda, M.; Winiarski, M. J.; Klimczuk, T.; Zaleska-Medynska, A. Photocatalytic Activity of Nitrogen Doped TiO2nanotubes Prepared by Anodic Oxidation: The Effect of Applied Voltage, Anodization Time and Amount of Nitrogen Dopant. *Appl. Catal. B Environ.* **2016**, *196* (October), 77–88.

(52) Hsu, S. J.; Lin, I. J. B. Synthesis of Gold Nanosheets through Thermolysis of Mixtures of Long Chain 1-Alkylimidazole and Hydrogen Tetrachloroaurate(III). *J. Chinese Chem. Soc.* **2009**, *56* (1), 98–106.

(53) Zhuang, H.; Lin, C.; Lai, Y.; Sun, L.; Li, J. Some Critical Structure Factors of Titanium Oxide Nanotube Array in Its Photocatalytic Activity Some Critical Structure Factors of Titanium Oxide Nanotube Array in Its Photocatalytic Activity. **2007**, No. December, 4735–4740.

(54) Li, X.; Liu, P.; Mao, Y.; Xing, M.; Zhang, J. Preparation of Homogeneous Nitrogen-Doped Mesoporous TiO2spheres with Enhanced Visible-Light Photocatalysis. *Appl. Catal. B Environ.* **2015**, *164*, 352–359.

(55) Liang, H.; Li, X. Effects of Structure of Anodic TiO2 Nanotube Arrays on Photocatalytic

MOST WIEDZY Downloaded from mostwiedzy.pl

Activity for the Degradation of 2,3-Dichlorophenol in Aqueous Solution. *J. Hazard. Mater.* **2009**, *162* (2–3), 1415–1422.

TOC/Abstract Graphic

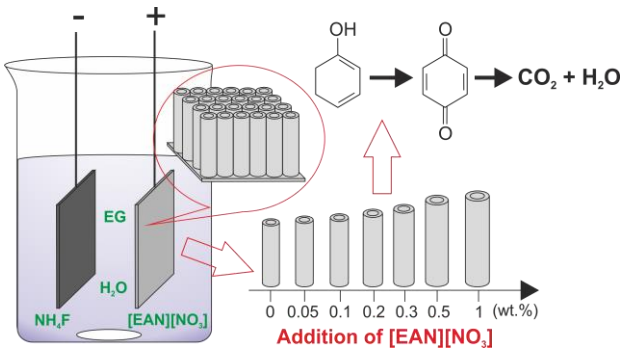

Synopsis

Study provides the framework for a new way to prepare TiO_2 NTs possessing tunable morphology and thus effectively utilize renewable energy source to solve environmental problems using heterogeneous photocatalysis processes.

MOST WIEDZY Downloaded from mostwiedzy.pl